A Compact Filtering 180° Hybrid

Chin-Kai Lin and Shyh-Jong Chung, *Senior Member, IEEE*

***Abstract*—A novel compact filtering 180° hybrid utilizing coupled resonators is presented. The equivalent-circuit structure is just like a bandpass filter, thus the frequency response is filter-like. The sum and difference port operations respectively correspond to the symmetric and antisymmetric states; therefore, isolation between sum and difference ports is accomplished by geometrical symmetry. The synthesis method of the filtering 180° hybrid is illustrated. The proposed structure is decomposed into one power divider and one balun, which are designed separately. A second-order filtering 180° hybrid prototype centered at 2.4 GHz with 0.2-dB Chebyshev equal-ripple response and 10% fractional bandwidth is demonstrated. The passband insertion loss is about $(3.0 + 0.7)$ dB, and the isolation between the sum and difference port is greater than 20 dB. Magnitude imbalance is less than 1 dB and phase imbalance is within 2°. Good agreement between simulation and experimental results is achieved.**

***Index Terms*—Baluns, bandpass filters, filter synthesis, 180° hybrids, power dividers.**

I. Introduction

SIZE reduction of microwave components is one of the constant challenging issues for RF engineers because of the ongoing miniaturization of portable devices. Multiple function design, which combines two or more components into one microwave device, is one of the popular approaches. The integrated designs reduce the number of microwave components, occupy less circuit area, and enhance overall circuit performance.

Bandpass filters appear in almost every microwave system. Thus, many studies on bandpass-filter-integrated components were investigated, such as power dividers [1], [2], balanced-to-unbalanced transformers (baluns) [3], [4], diplexers [5], and antennas [6]. In these designs, terminal ports are loaded by resonators that couple with each other for power transfer and phase control.

The 180° hybrid is another fundamental component in microwave circuits. In order to miniaturize it, there are several ways to attack this problem. In conventional design, four ports are bridged with transmission-line sections [7]. For miniaturizing the circuit size, the transmission-line sections are replaced either by folded lines [8], loaded lines [9], step-impedance resonators [10], composite left/right-hand transmission lines [11], phase inverters [12], or lumped elements [13]. A special design in [14] consists of two sets of coupled lines and a section of delay line. In those transmission-line-based structures, however, four transmission-line arms are supposed to be independent. When further miniaturization is applied, unwanted mutual coupling among arms are unavoidable, and thus degradation on performance occurs.

In another point of view, a 180° hybrid could be deconstructed into a power divider and a balun [15]. Thus, we could design those two components separately, and combine them into a single device. In the operation of waveguide magic-T [7], the symmetric mode corresponds to the power divider, while antisymmetric mode corresponds to the balun. In some designs [16], [17], the 180° hybrid is composed of the microstrip T-junctions (symmetric/unbalanced structure) and the slot line (antisymmetric/balanced structure). Therefore, geometrical symmetry is one of the points we could employ for isolating the power divider and balun functions.

Recently, some researches were attempting to implant the function of the bandpass filter into 180° hybrids [18], [19]. The resonator loaded hybrids was first proposed in [18]. However, the analysis was rough and the results were poor. This idea was later implemented using a printed circuit in [19]. Although the bandpass characteristics were good, the response was restricted to the maximally flat one. That is, it was optimized only at the center frequency. Notice that in [20], a 90° hybrid was also made up with coupled resonators. Nevertheless, this circuit lacks the function of a bandpass filter.

In this paper, we combine all the above-mentioned ideas and propose a novel filtering 180° hybrid. Four ports are loaded with resonators, and the interconnecting transmission lines are replaced with admittance inverters that provide $\pm 90°$ phase delay/advance. Geometrical symmetry is utilized for isolation between the sum and difference ports. The equivalent circuit is established and analyzed. It will be revealed from the analysis that the bandpass characteristics and the isolations among ports are theoretically achievable. The design guide is also obtained from those derivations. This paper is organized as follows. Section II illustrated the circuit structure and its operation principle. The equivalent circuit is analyzed in Section III, and the synthesis process and simulated results are presented in Section IV. Measurement results are exhibited in Section V and followed by a brief conclusion in Section VI.

II. Geometry and Operation Principle

The circuit layout and the detail dimensions of each part are shown in Fig. 1. The filtering 180° hybrid is printed on a 31-mil-thick Rogers RT/Duroid 5880 substrate with dielectric constant 2.2 and loss tangent 0.0009. In this study, a 180° hybrid with a second-order Chebyshev equal-ripple filter response is demonstrated.

Manuscript received March 21, 2011; revised August 16, 2011; accepted August 29, 2011. Date of publication October 28, 2011; date of current version December 14, 2011. This work was supported in part by the National Science Council, R.O.C., under Contract NSC 97-2221-E-009-041-MY3.

The authors are with the Institute of Communications Engineering, National Chiao Tung University, Hsinchu 300, Taiwan (e-mail: sjchung@cc.nctu.edu.tw).

Color versions of one or more of the figures in this paper are available online at http://ieeexplore.ieee.org.

Digital Object Identifier 10.1109/TMTT.2011.2169276

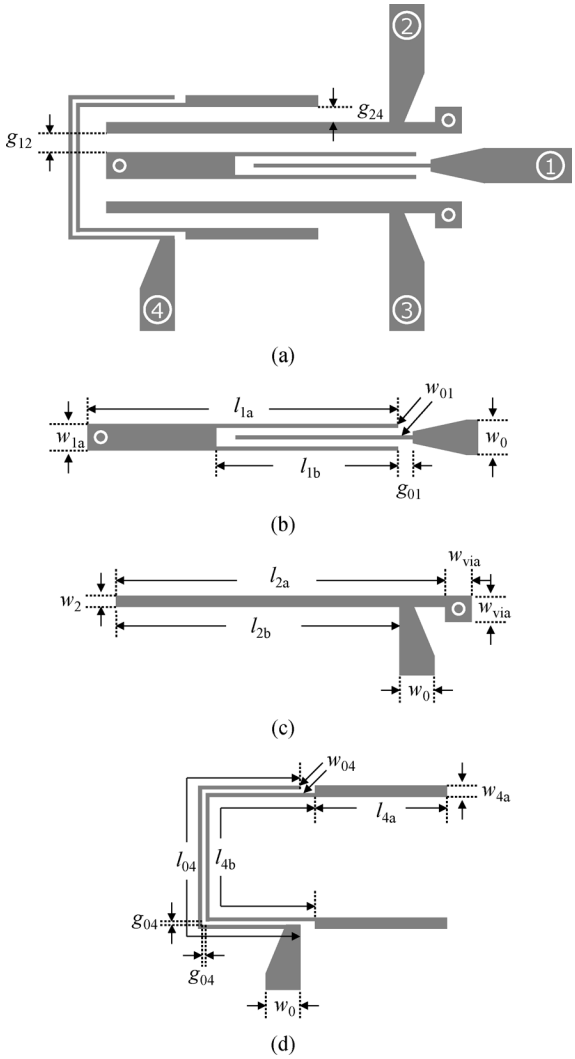

Fig. 1. Geometry of the filtering 180° hybrid and dimensions of each part. (a) Circuit layout. (b) Resonator 1 and its coupling section. (c) Resonators 2 and 3. (d) Resonator 4 and its coupling section.

Referring to Fig. 1(a), the filtering 180° hybrid consists of four microstrip resonators, which are fed by four feed lines labeled by the circled port numbers. Except for the port 4 feeding section, this circuit has a geometrical symmetry along the horizontal feeding line of port 1. Resonator 1 [see Fig. 1(b)] is a quarter-wavelength microstrip resonator with a via on its left and is excited by the inserted coupling Section 1. Resonator 2 [see Fig. 2(c)] is also a quarter-wavelength transmission-line resonator and is excited by the tapped microstrip line. Resonator 3 is the reflection of resonator 2, which is as well a quarter-wavelength resonator. Resonator 4 [see Fig. 1(d)] is a half-wavelength stepped-impedance resonator (SIR). The high impedance narrow width section is designed for enhancing the coupling with the feeding coupling Section 4. These four resonators are all operating at their fundamental modes with the same resonant frequency.

A 180° hybrid can be separated into two parts—one power divider and one balun [15]. When a signal is injected into port 1, resonator 1 is excited, with part of the signal coupled to both resonators 2 and 3. Due to geometrical symmetry, the equal magnitude and phase signals are then taken out from port 2 and 3, just as a *power divider* should do. The induced currents on resonator 2 and 3 would both couple to the nearby resonator 4. However, to excite the fundamental mode of resonator 4, an antisymmetric source is needed. Thus, the currents on resonators 2 and 3 cancel out each other, and then leave port 4 isolated.

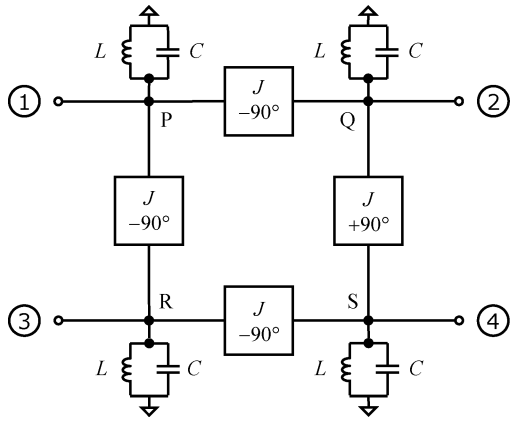

Fig. 2. Equivalent lumped circuit model of the filtering 180° hybrid.

When the signal is injected from port 4, another situation occurs. The current distribution of the half-wavelength resonance of resonator 4 is in an antisymmetric shape. Resonators 2 and 3 are then excited with equal magnitude, but opposite phase signals. With proper design, a *balun* could be achieved. These opposite currents on resonators 2 and 3 consequently couple to resonator 1 and cancel with each other. Thus, port 1 is isolated while ports 4, 2, and 3 act as a balun.

If the power divider (ports 1, 2, 3) and the balun (ports 4, 2, 3) are both designed with 3-dB power split ability, then, because of the reciprocity of a passive device, a signal incident from port 2 would also split in half into port 1 and port 4. The same argument also holds true for excitation from port 3.

According to the discussion above, in the passband, the structure in Fig. 1(a) has exactly the same functions of a 180° hybrid. In the out-of-band frequencies, the signals are reflected back to the input ports because the resonators are off resonance. Thus, the function of the bandpass filter is introduced.

III. Analysis

In this section, we establish and analyze the equivalent circuit for gaining some essential properties of the filtering 180° hybrid. A summary at the end of this section will reveal the design strategies and design steps.

Fig. 2 is the equivalent circuit of the filtering 180° hybrid. Four resonators are to be designed with the same external quality factor (Q_e) and resonant frequency (f_0). Thus, we use four identical parallel *LC* resonators to model these four microstrip resonators. The in-phase couplings of "resonator 1-to-2" and "resonator 1-to-3" are modeled by two interconnected -90° J-inverters (admittance inverters). The 180° out-of-phase couplings of "resonator 4-to-2" and "resonator 4-to-3" are modeled, respectively, by one $+90^\circ$ and one -90° J-inverters. The cross couplings between "resonator 2-to-3" and "resonator 1-to-4" are neglected in this model because the distances between them are relatively longer.

With some network analysis, one can derive the scattering matrix of the equivalent circuit in Fig. 2 as

$$[S] = \begin{bmatrix} \alpha & \beta & \beta & 0 \\ \beta & \alpha & 0 & -\beta \\ \beta & 0 & \alpha & \beta \\ 0 & -\beta & \beta & \alpha \end{bmatrix} \quad \begin{matrix} \text{Power divider} \\ \\ \\ \text{Balun} \end{matrix} \tag{1}$$

with the matrix elements α and β being

$$\alpha = -\frac{2J^2 - Y_0^2 + Y_R^2}{2J^2 + (Y_0 + Y_R)^2} \tag{2}$$

$$\beta = -\frac{2jY_0J}{2J^2 + (Y_0 + Y_R)^2} \tag{3}$$

where Y_0 is the admittance of the port, and Y_R is the admittance of the *LC* resonator, which is a function of frequency f,

$$Y_R = j(2\pi f)C + \frac{1}{j(2\pi f)L}. \tag{4}$$

Notice that the matrix elements α and β are both functions of frequency.

If we set $Y_R = 0$ (without loading resonators), and $J = Y_0/\sqrt{2}$, then $\alpha = 0$ and $\beta = -j/\sqrt{2}$, and (1) reduces to the S-matrix of a conventional 180° hybrid at its center frequency.

Observing the diagonal elements in (1), these four ports have the same reflection coefficients ($S_{11} = S_{22} = S_{33} = S_{44} = \alpha$) while the other ports are terminated. From the first column of (1), $S_{21} = S_{31} = \beta$. That is, when a source is applied on port 1, ports 2 and 3 have the equal output signal, just as the function of a power divider. On the other hand, referring to the fourth column of (1), $S_{34} = -S_{24} = \beta$, i.e., the output ports 2 and 3 have the differential signals. Thus, port 4, 2, and 3 act like a balun. In addition, there are theoretical infinite isolations between ports 1, 4 and ports 2, 3 for all frequencies ($S_{14} = S_{23} = S_{32} = S_{41} = 0$).

For the circuit model in Fig. 2, when a voltage signal injects into port 1, there are two paths to reach port 4, one is path PQS and the other is path PRS. On path PQS, there are one "$J + 90°$" and one "$J - 90°$" inverters so the signal accumulates the phase of 0°. Meanwhile, the signal from path PRS has the phase of $-180°$ accumulated due to two "$J - 90°$" inverters. These two signals cancel out each other and result in zero voltage (a virtual short circuit) on node S. Thus, isolation between ports 1 and 4 ($S_{41} = 0$) is achieved as observed in (1). Whether from nodes Q or R, if we look toward node S across the J-inverters, we will see infinite impedance (open circuited) since node S is virtually shorted. It means that we can remove resonator 4, port 4, and the "R-to-S" and "Q-to-S" J-inverters without affecting the operation of the power divider. The resultant circuit is shown in Fig. 3(a). By the same argument, in Fig. 2, the balun (ports 4, 2, 3) works without resonator 1, port 1, and the "P-to-Q" and "P-to-R" J-inverters, as depicted in Fig. 3(b). The S-matrices of the power divider and the balun are derived as

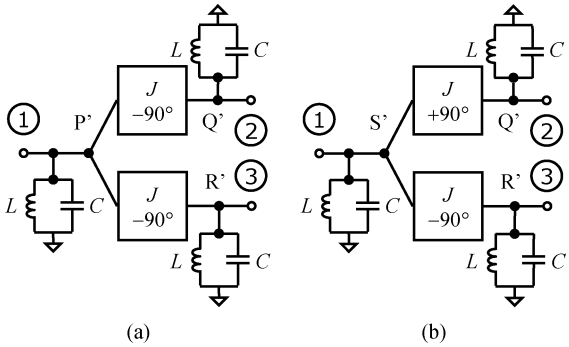

Fig. 3. Decomposition of the filtering 180° hybrid equivalent circuit. (a) Filtering power divider. (b) Filtering balun.

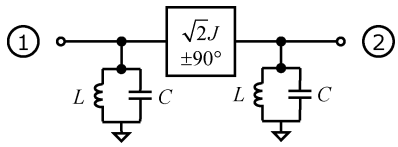

Fig. 4. Equivalent circuit of the coupled-resonator bandpass filter.

$$\left[S^{\text{divider}}\right] = \begin{bmatrix} \alpha & \beta & \beta \\ \beta & \alpha+\gamma & -\gamma \\ \beta & -\gamma & \alpha+\gamma \end{bmatrix} \tag{5}$$

$$\left[S^{\text{balun}}\right] = \begin{bmatrix} \alpha & -\beta & \beta \\ -\beta & \alpha+\gamma & \gamma \\ \beta & \gamma & \alpha+\gamma \end{bmatrix} \tag{6}$$

with γ being

$$\gamma = \frac{2Y_0J^2}{(Y_0 + Y_R)\left[2J^2 + (Y_0 + Y_R)^2\right]}. \tag{7}$$

Comparing (5) and the power divider part of (1), the first column and the first row are identical. It indicates that the power-dividing function is kept, although isolation between ports 2 and 3 is destroyed. Similarly in (6), the function of the balun also holds. Moreover, since $S_{23}^{\text{divider}} = S_{32}^{\text{divider}} = -S_{23}^{\text{balun}} = -S_{32}^{\text{balun}} = -\gamma$, when we combine the power divider and balun, the isolation between ports 2 and 3 will be retained. These properties imply that the power divider and the balun can be designed separately, and when we combine these two elements, the same responses remain.

From point P' in Fig. 3(a), whether we look toward port 2 or port 3, which are connected in parallel, the input admittances are the same. The power divider in Fig. 3(a) can be further reduced to Fig. 4 with the same port 1 reflection coefficient. The admittance increases up to $\sqrt{2}J$ because of twice the coupling level. The circuit in Fig. 4 is exactly a second-order coupled-resonator bandpass filter with the S-parameter

$$\left[S^{\text{filter}}\right] = \begin{bmatrix} \alpha & \pm\sqrt{2}\beta \\ \pm\sqrt{2}\beta & \alpha \end{bmatrix}. \tag{8}$$

The balun in Fig. 3(c) can also be reduced to the filter model in Fig. 4.

Since the circuit in Fig. 4 is a coupled-resonator bandpass filter, it can be design by the conventional synthesis technology

[21]. Take the second-order Chebyshev equal-ripple response for example, with the specified center frequency (f_0), ripple level (L_a) (dB), and fractional bandwidth (Δ), the element values can be calculated

$$L = \frac{\sinh(\mu/4)}{\sqrt{2}} \frac{\Delta}{2\pi f_0 Y_0} \tag{9}$$

$$C = \frac{\sqrt{2}}{\sinh(\mu/4)} \frac{Y_0}{2\pi f_0 \Delta} \tag{10}$$

$$J = \frac{1}{\sqrt{2}} Y_0 \coth(\mu/4) \tag{11}$$

where μ is

$$\mu = \ln\left[\coth\left(\frac{\ln 10}{40} \times L_a\,(\text{dB})\right)\right]. \tag{12}$$

Note that the equivalent circuit of the 90° hybrid in [20] has infinite isolation only at its center frequency. At other frequencies, the input port and the isolation port seriously interfere with each other. Accordingly, the structure in [20] essentially does not have a bandpass filter response.

In summary, the design procedure of the proposed filtering Chebyshev equal-ripple 180° hybrid is listed as follows.

Step 1) Get the second-order bandpass filter specifications, including the center frequency (f_0), the fractional bandwidth (Δ), the ripple level [L_a (dB)], and the port admittance (Y_0).

Step 2) Evaluate the element values L, C, and J by (9)–(12).

Step 3) Design four resonators with the same external quality factor Q_e,

$$Q_e = \frac{1}{Y_0}\sqrt{\frac{C}{L}}. \tag{13}$$

Step 4) Separately design the filtering power divider and the balun in Fig. 3 using the bandpass filter synthesis method. The coupling coefficients between resonators are

$$M_{ij} = \pm\frac{\sqrt{2}J}{2\pi f_0}\frac{1}{C}. \tag{14}$$

When the "+" sign is taken when $(i,j) = (1,2),(1,3)$, and $(1,4)$, while the "−" sign is taken when $(i,j) = (2,4)$.

Step 5) Arrange the power divider and the balun, and the four port filtering 180° hybrid is completed.

IV. Synthesis

Based on the discussion above, the filtering 180° hybrid could be decomposed into one power divider and one balun. Thus, our strategy is to separately design these two components, and then combine them into one. Note that the full-wave simulation throughout this work is done using IE3D [22].

In this case, we design a 50-Ω ($Y_0 = 0.02$ S) filtering 180° hybrid centered at 2.4 GHz (f_0) with second-order Chebyshev 0.2-dB [L_a (dB)] equal-ripple response and 10% fractional bandwidth (Δ). The parameter values of the equivalent circuit in Fig. 2 are then evaluated using (9)–(12): $Y_0 = 0.02$ S, $C = 13.8$ pF, $L = 0.32$ nH, $J = 0.017$ S.

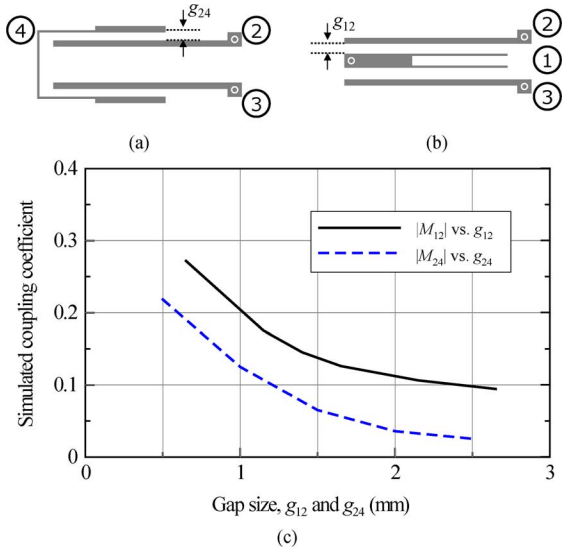

Fig. 5. Coupling coefficient tests. (a) Circuit layout for extracting M_{12}. (b) Circuit layout for extracting M_{24}. (c) Simulated coupling coefficients as functions of gap sizes.

A. External Quality Factors

We need the resonant frequency and external quality factor to design the resonators. The resonant frequency for all four resonators is $f_0 = 2.4$ GHz. Substitute the previously derived element values into (13), we get $Q_e = 10.4$.

The layouts of the resonators are shown in Fig. 1(b)–(d). The resonant frequency could be easily reached by adjusting the lengths of resonators (l_{1a}, l_{2a}, and $l_{4a} + l_{4b}$). For resonators 1 and 4, the external quality factor Q_e is determined by the gap between the resonators and coupling sections, g_{01} and g_{04}. With stronger coupling, we get lower Q_e. For resonators 2 and 3, when the tap position is closer to the via (larger l_{2b}), Q_e increases. The resonator design is a common technology [21]; thus we neglect the description of the detail tuning process. The dimensions labeled in Fig. 1(b)–(d) are $w_0 = 2.46$ mm, $w_{1a} = 1.5$ mm, $l_{1a} = 21.5$ mm, $l_{1b} = 12.5$ mm, $w_{01} = 0.3$ mm, $l_{01} = 12.5$ mm, $w_{via} = 1.5$ mm, $w_2 = 0.8$ mm, $l_{2a} = 22.8$ mm, and $l_{2b} = 18.25$ mm, $w_{04} = 0.3$ mm, $l_{04} = 24.8$ mm, $w_{4a} = 0.8$ mm, $l_{4a} = 9.2$ mm, $l_{4b} = 22.6$ mm, $g_{01} = 1.0$ mm, and $g_{04} = 0.3$ mm.

B. Coupling Coefficients

In Fig. 5, we perform some tests for extracting the coupling coefficients. Fig. 5(a) and (b) depicts the full-wave simulation models for extracting M_{12} and M_{24}, respectively, and Fig. 5(c) shows the simulation results.

The power divider includes resonators 1–3. Due to geometrical symmetry, output balance is automatically achieved. According to (14), $|M_{12}| = 0.116$ in this study. The coupling between resonators 1–3 is determined by the gap g_{12} in Fig. 5(a). As shown in Fig. 5(c) (solid line), the coupling coefficient M_{12}

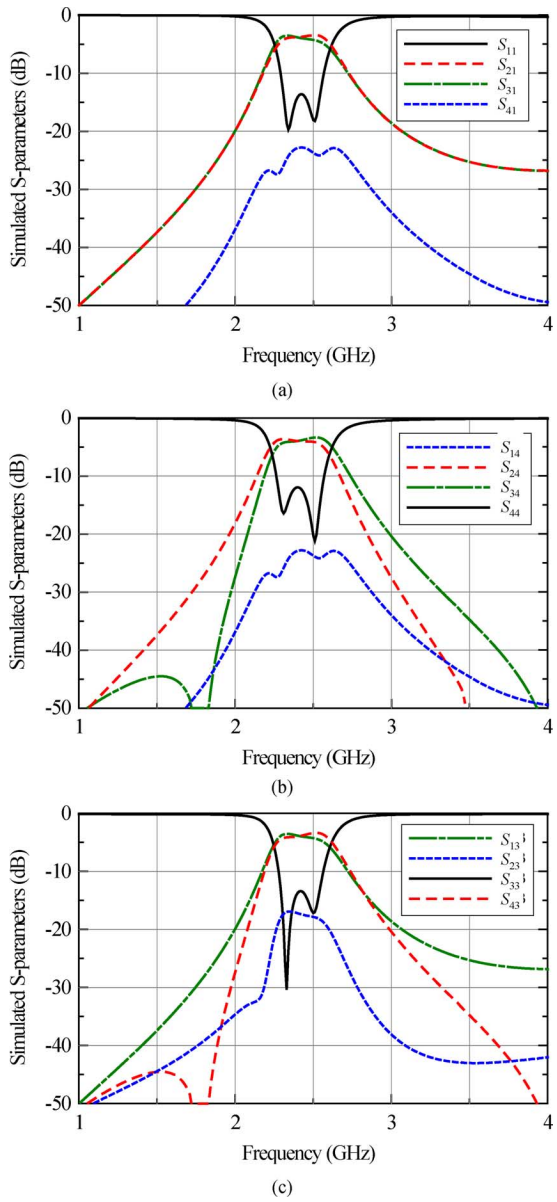

Fig. 6. Simulated S-parameters with signal incident from: (a) port 1 (sum port), (b) port 4 (difference port), and (c) port 3.

increases as g_{12} decreases. When $g_{12} = 1.9$ mm, we get the required coupling level.

Likewise, the balun design includes resonators 4, 2, and 3 [see Fig. 5(b)]. The coupling coefficient M_{24} varies with the gap g_{24}. Also in Fig. 5(c) (dashed line), the required coupling coefficient $|M_{24}| = 0.116$ is gotten around $g_{24} = 1.1$ mm.

C. Synthesis

After combining the power divider and balun, the final dimensions of the structure in Fig. 1 are $w_0 = 2.46$ mm, $w_{1a} = 1.5$ mm, $l_{1a} = 21.5$ mm, $l_{1b} = 12.5$ mm, $w_{01} = 0.3$ mm, $w_{via} = 1.5$ mm, $w_2 = 0.8$ mm, $l_{2a} = 22.8$ mm, $l_{2b} = 18.25$ mm, $w_{04} = 0.3$ mm, $l_{04} = 24.8$ mm, $w_{4a} = 0.8$ mm, $l_{4a} = 9.2$ mm, $l_{4b} = 22.6$ mm, $g_{01} = 1.0$ mm, $g_{04} = 0.3$ mm, $g_{12} = 1.65$ mm, and $g_{24} = 1.0$ mm.

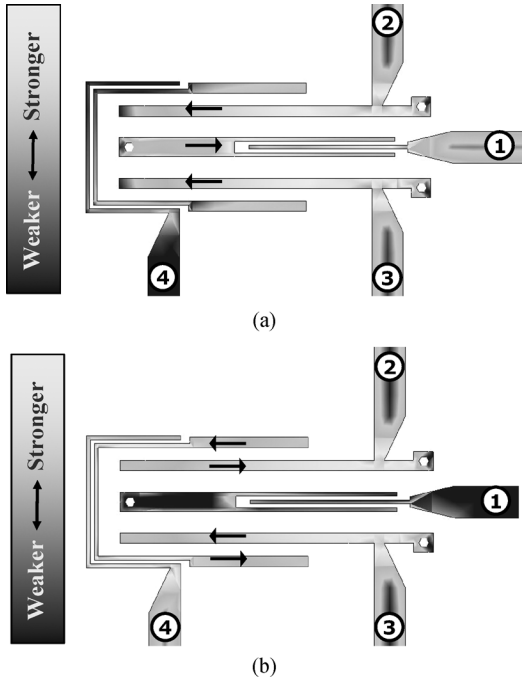

Fig. 7. Averaged current distribution at passband center frequency 2.4 GHz while signal incident form: (a) port 1 (symmetric state) and (b) port 4 (antisymmetric state).

Fig. 6(a)–(c) exhibits the full-wave simulated S-parameters with the signals injected from ports 1, 4, and 2, respectively. All ports have almost the identical return-loss response, just as what we expected from (5). The minimum return loss in the passband is about 13 dB, and there are two dips within the passband. The output port responses have fast roll-off at the band edge. Good out-of-band rejection can be observed from the results. The isolations between ports (S_{14} and S_{23}) are around 20 dB.

Notice that, for S_{34}, there are two transmission zeros, one is at 1.8 GHz and another is at 4 GHz. The lower frequency transmission zero at 1.8 GHz is because the microstrip section $(l_{4a} + l_{4b})$ in Fig. 1(d) reaches half-wavelength resonance, and the higher frequency transmission zero at 3.9 GHz is due to the half-wavelength resonance of the port 4 coupling section with length l_{04}. With the same reason, S_{42} has also a transmission zero around 3.9 GHz.

D. Current Distribution

Fig. 7 shows the plots of current distributions. From these current distribution diagrams for the symmetric and antisymmetric states, the principle for isolation between ports 1 and 4 can be clearly understood. Fig. 7(a) is plotted under the situation that port 1 is excited while other ports are terminated. Resonator 1 has, of course, the strongest current flow and then couples to the neighboring resonators 2 and 3. The induced current on resonators 2 and 3 are in the same direction so that the half-wavelength resonator 4 is not able to be excited. Thus, there is no signal coming out from port 4.

When the source is incident from port 4, referring to Fig. 7(b), ports 2 and 3 are coupled with equal magnitude, but 180° out-of-phase signals. These destructive signals cancel out each other on resonator 1. Therefore, isolation is realized.

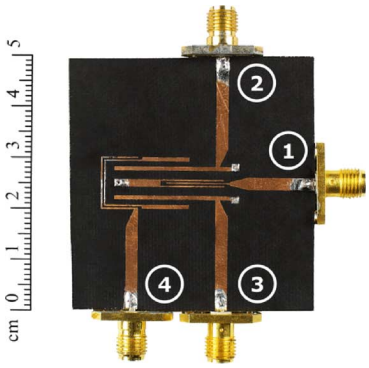

Fig. 8. Photograph of the fabricated filtering 180° hybrid.

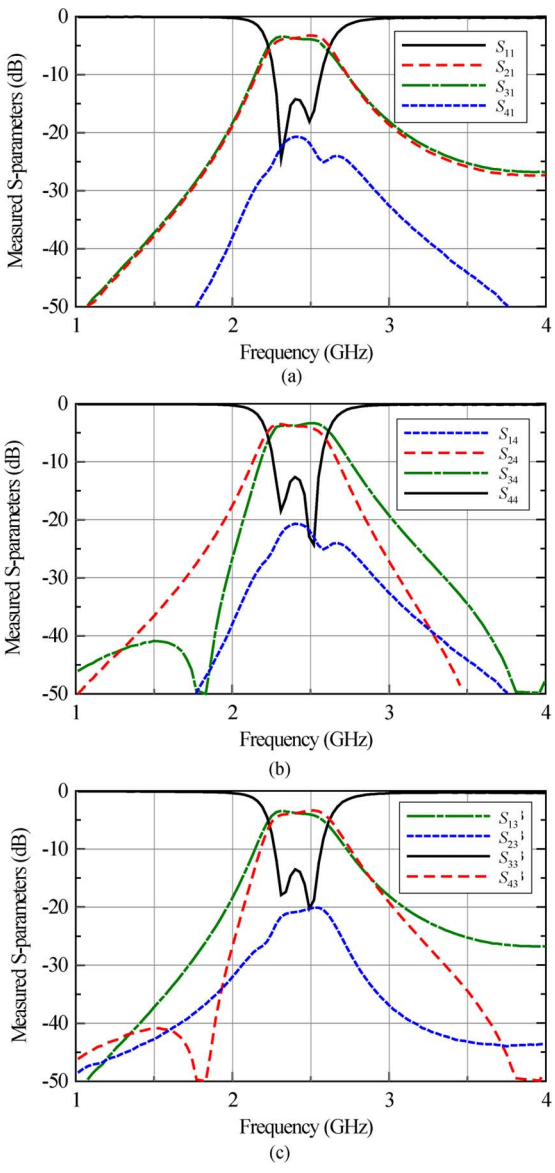

Fig. 9. Measured S-parameters with signal incident from: (a) port 1 (sum port), (b) port 4 (difference port), and (c) port 3.

V. Measurement Results

Fig. 8 exhibits a photograph of the fabricated filtering 180° hybrid. Fig. 9(a)–(c) shows the measurement results. The measured results are almost identical to the simulated ones, except

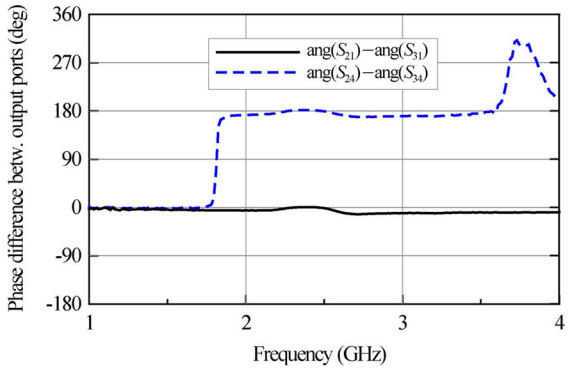

Fig. 10. Unwrapped phase differences between output ports.

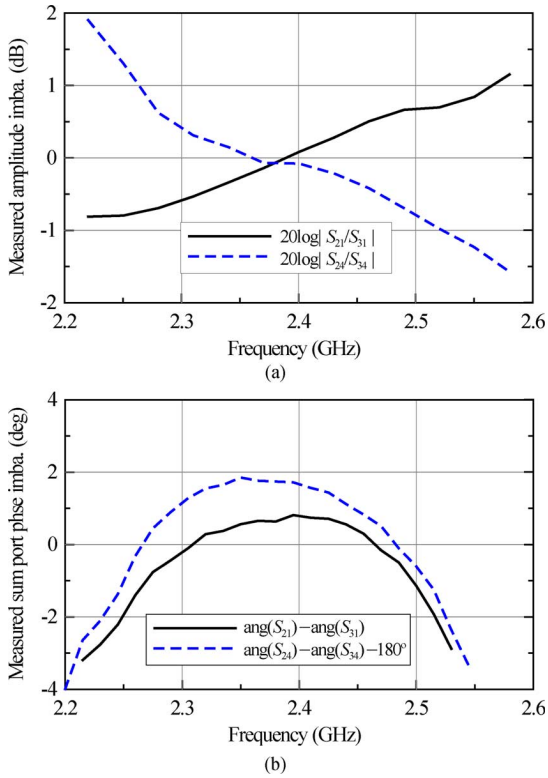

Fig. 11. Measured: (a) amplitude and (b) phase imbalances of the sum (solid lines) and difference port (dashed lines) signals.

that the measured S_{23} in the passband is lower than -20 dB, while the simulated S_{23} is around -18 dB. The passband insertion loss is about $(3.0 + 0.7)$ dB.

Fig. 10 shows the unwrapped phase differences between output ports (ports 2 and 3) for both port 1 and port 4 incidences. Intuitively, because of geometrical symmetry, the phase difference for port 1 incidence (solid line) is close to zero for all frequency. Some disturbance occurs because of the asymmetric port 4 coupling section.

For the case of port 4 incidence (dashed line), below 1.8 GHz, resonator 4 is out-of-resonance. At such low frequencies, the long-wavelength signal almost uniformly distributes on resonator 4, resulting in in-phase coupling to ports 2 and 3. At frequency higher than 1.8 GHz, the resonance begins and a transmission zero for S_{34} occurs (see Fig. 9); the phase difference abruptly jumps to 180° due to the transmission zero for S_{34} at 1.8 GHz. It keeps around 180° phase difference all the

way to about 3.9 GHz where there is another transmission zero for S_{34}. However, the out-of-band signal output level is rather low, thus, the phase difference is not so important at all.

Fig. 11 shows the magnified plot of imbalance response both in magnitude and phase. When the source incidents from port 1, the passband (2.28–2.52 GHz) output magnitude and phase imbalance are within 0.7 dB and 2°, respectively. With signal applied from port 4, the output magnitude and phase imbalance are within 1.0 dB and 2°, respectively.

VI. Conclusion

A novel compact filtering 180° hybrid utilizing coupled resonators is presented. Several properties of the filtering 180° hybrid is obtained by analyzing the equivalent circuit. The filtering 180° hybrid is decomposed into one power divider and one balun, which are separately designed through a filter synthesis process. Isolation between sum and difference ports is achieved by geometrical symmetry and resonator mode selection. A second-order prototype centered at 2.4 GHz with a 0.2-dB Chebyshev equal-ripple response and 10% fractional bandwidth was demonstrated. The measured passband insertion loss is about $(3.0 + 0.7)$ dB, and isolation is greater than 20 dB. Magnitude imbalance is within 1-dB variation and phase imbalance is within 2°. Good agreement between simulation and experiment results is shown.

It is believed that the proposed architecture is suitable for further size reduction, such as low-temperature co-fired ceramic (LTCC) and integrated circuit (IC) designs. In the conventional transmission line-based reduced-sized 180° hybrid designs, four transmission line arms are supposed to be operated independently. However, unwanted mutual coupling between those arms happens when circuit size reduces. When those arms are replaced by electromagnetic coupling between resonators, the consideration on isolation among those arms vanishes. Instead, with the stronger coupling, a wider operation passband bandwidth can be achieved. Dual-band operation can be easily accomplished by adopting the existing SIR-filter techniques. For enhancing the selectivity and isolation, higher order filter structure may be considered.

References

[1] K. Song and Q. Xue, "Novel ultra-wideband (UWB) multilayer slotline power divider with bandpass response," *IEEE Microw. Wireless Compon. Lett.*, vol. 20, no. 1, pp. 13–15, Jan. 2010.

[2] P. K. Singh, S. Basu, and Y. H. Wang, "Coupled line power divider with compact size bandpass response," *Electron. Lett.*, vol. 45, no. 17, pp. 892–894, Aug. 2009.

[3] K.-T. Chen and S.-J. Chung, "A novel compact balanced-to-unbalanced low-temperature co-fired ceramic bandpass filter with three coupled lines configuration," *IEEE Trans. Microw. Theory Tech.*, vol. 56, no. 7, pp. 1714–1720, Jul. 2008.

[4] C. H. Wu, C. H. Wang, S. Y. Chen, and C. H. Chen, "Balanced-to-unbalanced bandpass filters and the antenna application," *IEEE Trans. Microw. Theory Tech.*, vol. 56, no. 11, pp. 2474–2482, Nov. 2008.

[5] C. W. Tang and S. F. You, "Design methodologies of LTCC bandpass filters, diplexer, and triplexer with transmission zeros," *IEEE Trans. Microw. Theory Tech.*, vol. 54, no. 2, pp. 717–723, Feb. 2006.

[6] C. T. Chuang and S.-J. Chung, "Synthesis and design of a new printed filtering antenna," *IEEE Trans. Antennas Propag.*, to be published.

[7] D. M. Pozar, *Microwave Engineering*, 3rd ed. New York: Wiley, 2005, ch. 7.

[8] R. K. Settaluri, G. Sundberg, A. Weisshaar, and V. K. Tripathi, "Compact folded line rat-race hybrid couplers," *IEEE Trans. Microw. Guided Wave Lett.*, vol. 10, no. 2, pp. 61–63, Feb. 2000.

[9] C. L. Hsu, J. T. Kuo, and C. W. Chang, "Miniaturized dual-band hybrid couplers with arbitrary power division ratios," *IEEE Trans. Microw. Theory Tech.*, vol. 57, no. 1, pp. 149–156, Jan. 2009.

[10] J. T. Kuo, J. S. Wu, and Y. C. Chiou, "Miniaturized rat race coupler with suppression of spurious passband," *IEEE Microw. Wireless Compon. Lett.*, vol. 17, no. 1, pp. 46–48, Jan. 2007.

[11] I. H. Lin, M. DeVincentis, C. Caloz, and T. Itoh, "Arbitrary dual-band components using composite right/left-handed transmission lines," *IEEE Trans. Microw. Theory Tech.*, vol. 52, no. 4, pp. 1142–1149, Apr. 2004.

[12] B. R. Heimer, L. Fan, and K. Chang, "Uniplanar hybrid couplers using asymmetrical coplanar striplines," *IEEE Trans. Microw. Theory Tech.*, vol. 45, no. 12, pp. 2234–2240, Dec. 1997.

[13] C. H. Tseng, "Compact LTCC rat-race couplers using multilayered phase-delay and phase-advance T-equivalent sections," *IEEE Trans. Adv. Packag.*, vol. 33, no. 2, pp. 543–551, May 2010.

[14] V. Napijalo and B. Kearns, "Multilayer 180° coupled line hybrid coupler," *IEEE Trans. Microw. Theory Tech.*, vol. 56, no. 11, pp. 2525–2535, Nov. 2008.

[15] K. S. Ang and Y. C. Leong, "Converting baluns into broadband impedance-transforming 180° hybrids," *IEEE Trans. Microw. Theory Tech.*, vol. 50, no. 8, pp. 1990–1995, Aug. 2002.

[16] K. U-yen, E. J. Wollack, J. Papapolymerou, and J. Laskar, "A broadband planar magic-T using microstrip-slotline transitions," *IEEE Trans. Microw. Theory Tech.*, vol. 56, no. 1, pp. 172–177, Jan. 2008.

[17] N. Yang, C. Caloz, and K. Wu, "Broadband compact 180° hybrid derived from the Wilkinson divider," *IEEE Trans. Microw. Theory Tech.*, vol. 58, no. 4, pp. 1030–1037, Apr. 2010.

[18] H. Uchida, N. Yoneda, Y. Konishi, and S. Makino, "Bandpass directional couplers with electromagnetically-coupled resonators," in *IEEE MTT-S Int. Microw. Symp. Dig.*, 2006, pp. 1563–1566.

[19] W.-H. Wang, T.-M. Shen, T.-Y. Huang, and R.-B. Wu, "Miniaturized rat-race coupler with bandpass response and good stopband rejection," in *IEEE MTT-S Int. Microw. Symp. Dig.*, 2009, pp. 709–712.

[20] W. L. Chang, T. Y. Huang, T. M. Shen, B. C. Chen, and R. B. Wu, "Design of compact branch-line coupler with coupled resonators," in *Proc. Asia–Pacific Microw. Conf.*, 2007, pp. 1–4.

[21] J. S. Hong and M. J. Lancaster, *Microstrip Filters for RF/Microwave Applications*. New York: Wiley, 2001.

[22] IE3D Simulator. Zeland Softw. Inc., Fremont, CA, Jan. 1997.

Chin-Kai Lin was born in Keelung, Taiwan. He received the B.S. and M.S. degree in physics from National Tsing Hua University, Hsinchu, Taiwan, in 2004 and 2006, respectively, and is currently working toward the Ph.D. degree in communication engineering at National Chiao Tung University, Hsinchu, Taiwan.

His current research interests include design of antennas and microwave circuits.

Shyh-Jong Chung (M'92–SM'06) was born in Taipei, Taiwan. He received the B.S.E.E. and Ph.D. degrees from National Taiwan University, Taipei, Taiwan, in 1984 and 1988, respectively.

Since 1988, he has been with the Department of Communication Engineering, National Chiao Tung University, Hsinchu, Taiwan, where he is currently a Professor and serves as the Director of the Institute of Communication Engineering. From September 1995 to August 1996, he was a Visiting Scholar with the Department of Electrical Engineering, Texas A&M University, College Station. His areas of interest include the design and applications of active and passive planar antennas, low-temperature cofired ceramic (LTCC)-based RF components and modules, packaging effects of microwave circuits, vehicle collision-warning radars, and communications in intelligent transportation systems (ITSs).

Dr. Chung was the treasurer of IEEE Taipei Section (2001–2003) and chairman of IEEE Microwave Theory and Techniques Society (IEEE MTT-S) Taipei Chapter (2005–2007). He was the recipient of both the Outstanding Electrical Engineering Professor Award of the Chinese Institute of Electrical Engineering and the Teaching Excellence Awards of National Chiao Tung University in 2005.